A journal of world insect systematics

INSECTA MUNDI

0852

A new *Vaejovis* C.L. Koch from the Sierra Madre Occidental of Durango, Mexico (Scorpiones: Vaejovidae)

Jessica S. Azzinnari

Department of Life, Earth, & Environmental Sciences, West Texas A&M University, WTAMU Box 60808, Canyon, TX 79016-0001

Robert W. Bryson Jr.

Department of Biology & Burke Museum of Natural History and Culture, University of Washington, Box 351800, Seattle, WA 98195-1800

Matthew R. Graham

Department of Biology, Eastern Connecticut State University, 83 Windham Street, Willimantic, CT 06226.

Carlos Solís-Rojas

Laboratorio de Entomología y Artrópodos, Colección Aracnológica, Facultad de Ciencias Biológicas, Universidad Autónoma de Nuevo León, Apdo Postal 105-F, San Nicolas de los Garza, N.L. C.P. 66450 Mexico

W. David Sissom

Department of Life, Earth, & Environmental Sciences, West Texas A&M University, WTAMU Box 60808, Canyon, TX 79016-0001

Date of issue: February 26, 2021

Center for Systematic Entomology, Inc., Gainesville, FL

Azzinnari JS, Bryson RW Jr., Graham MR, Solís-Rojas C, Sissom WD. 2021. A new *Vaejovis* C.L. Koch from the Sierra Madre Occidental of Durango, Mexico (Scorpiones: Vaejovidae). Insecta Mundi 0852: 1–12.

Published on February 26, 2021 by
Center for Systematic Entomology, Inc.
P.O. Box 141874
Gainesville, FL 32614-1874 USA
http://centerforsystematicentomology.org/

Insecta Mundi is a journal primarily devoted to insect systematics, but articles can be published on any non-marine arthropod. Topics considered for publication include systematics, taxonomy, nomenclature, checklists, faunal works, and natural history. Insecta Mundi will not consider works in the applied sciences (i.e. medical entomology, pest control research, etc.), and no longer publishes book reviews or editorials. Insecta Mundi publishes original research or discoveries in an inexpensive and timely manner, distributing them free via open access on the internet on the date of publication.

Insecta Mundi is referenced or abstracted by several sources, including the Zoological Record and CAB Abstracts. Insecta Mundi is published irregularly throughout the year, with completed manuscripts assigned an individual number. Manuscripts must be peer reviewed prior to submission, after which they are reviewed by the editorial board to ensure quality. One author of each submitted manuscript must be a current member of the Center for Systematic Entomology.

Guidelines and requirements for the preparation of manuscripts are available on the Insecta Mundi website at http://centerforsystematicentomology.org/insectamundi/

Printed copies (ISSN 0749-6737) annually deposited in libraries

Florida Department of Agriculture and Consumer Services, Gainesville, FL, USA
The Natural History Museum, London, UK
National Museum of Natural History, Smithsonian Institution, Washington, DC, USA
Zoological Institute of Russian Academy of Sciences, Saint-Petersburg, Russia

Electronic copies (Online ISSN 1942-1354) in PDF format

Archived digitally by Portico
Florida Virtual Campus: http://purl.fcla.edu/fcla/insectamundi
University of Nebraska-Lincoln, Digital Commons: http://digitalcommons.unl.edu/insectamundi/
Goethe-Universität, Frankfurt am Main: http://nbn-resolving.de/urn/resolver.pl?urn:nbn:de:hebis:30:3-135240

0852: 1–12 **INSECTA MUNDI** 2021

A new *Vaejovis* C.L. Koch from the Sierra Madre Occidental of Durango, Mexico (Scorpiones: Vaejovidae)

Jessica S. Azzinnari

Department of Life, Earth, & Environmental Sciences, West Texas A&M University, WTAMU Box 60808, Canyon, TX 79016-0001
jsazzinnari@yahoo.com

Robert W. Bryson Jr.

Department of Biology & Burke Museum of Natural History and Culture, University of Washington, Box 351800, Seattle, WA 98195-1800
brysonjr@uw.edu

Matthew R. Graham

Department of Biology, Eastern Connecticut State University, 83 Windham Street, Willimantic, CT 06226.
grahamm@easternct.edu

Carlos Solís-Rojas

Laboratorio de Entomología y Artrópodos, Colección Aracnológica, Facultad de Ciencias Biológicas, Universidad Autónoma de Nuevo León, Apdo Postal 105-F, San Nicolas de los Garza, N.L. C.P. 66450 Mexico

W. David Sissom

Department of Life, Earth, & Environmental Sciences, West Texas A&M University, WTAMU Box 60808, Canyon, TX 79016-0001
dsissom@wtamu.edu

Abstract. A new montane species of *Vaejovis* C.L. Koch (Scorpiones: Vaejovidae) is described from the Sierra Madre Occidental of Durango, Mexico. *Vaejovis baggins* Azzinnari, Bryson, Graham, Solís-Rojas, and Sissom, **new species**, is similar to *mexicanus* group species in the mountain range, including *V. montanus* Graham and Bryson, *V. sierrae* Sissom, Graham, Donaldson, and Bryson, and *V. mcwesti* Sissom, Graham, Donaldson, and Bryson, but differs from these species based on aspects of body size, pedipalp carination, chelae granulation, morphometrics, and setal patterns on the metasoma. A molecular clock estimate indicates that the new species shared a common ancestor with *V. mcwesti* during the late Miocene or Pliocene.

Key words. Scorpion, systematics, *Vaejovis mcwesti*, *Vaejovis mexicanus* group, *Vaejovis montanus*, *Vaejovis sierrae*.

ZooBank registration. urn:lsid:zoobank.org:pub:5D29AB72-85CE-409D-A9B2-B3C6162CAD81

Introduction

The *mexicanus* group of the genus *Vaejovis* C.L. Koch was first established by Hoffmann (1931). Species of this group are typically found at high elevations among montane pine-oak habitat (Sissom 2000). Until recently, only one species of the *mexicanus* group was known from the main massif of the Sierra Madre Occidental, the largest mountain range in Mexico (Ferrusquía-Villafranca et al. 2005; Graham and Bryson 2010). In 2016 two more species were described from the Sierra Madre Occidental (Sissom et al. 2016), bringing the total number of species in the *mexicanus* group known from this mountain range to three: *Vaejovis montanus* Graham and Bryson, *Vaejovis sierrae* Sissom, Graham, Donaldson, and Bryson, and *Vaejovis mcwesti* Sissom, Graham, Donaldson, and Bryson. The latter two species are known from localities in central and southern Durango (Fig. 1). Based on genetic data in a previous study (Bryson et al. 2013) and morphological data presented herein, a third distinct yet undescribed species occurs in the mountainous region between the ranges of *V. mcwesti* and *V. sierrae*. Here we describe this third species and compare it to other *mexicanus* group species in the Sierra Madre Occidental. The new species is placed in the *mexicanus* group based on diagnostic characters set forth by Contreras-Félix and Francke (2019).

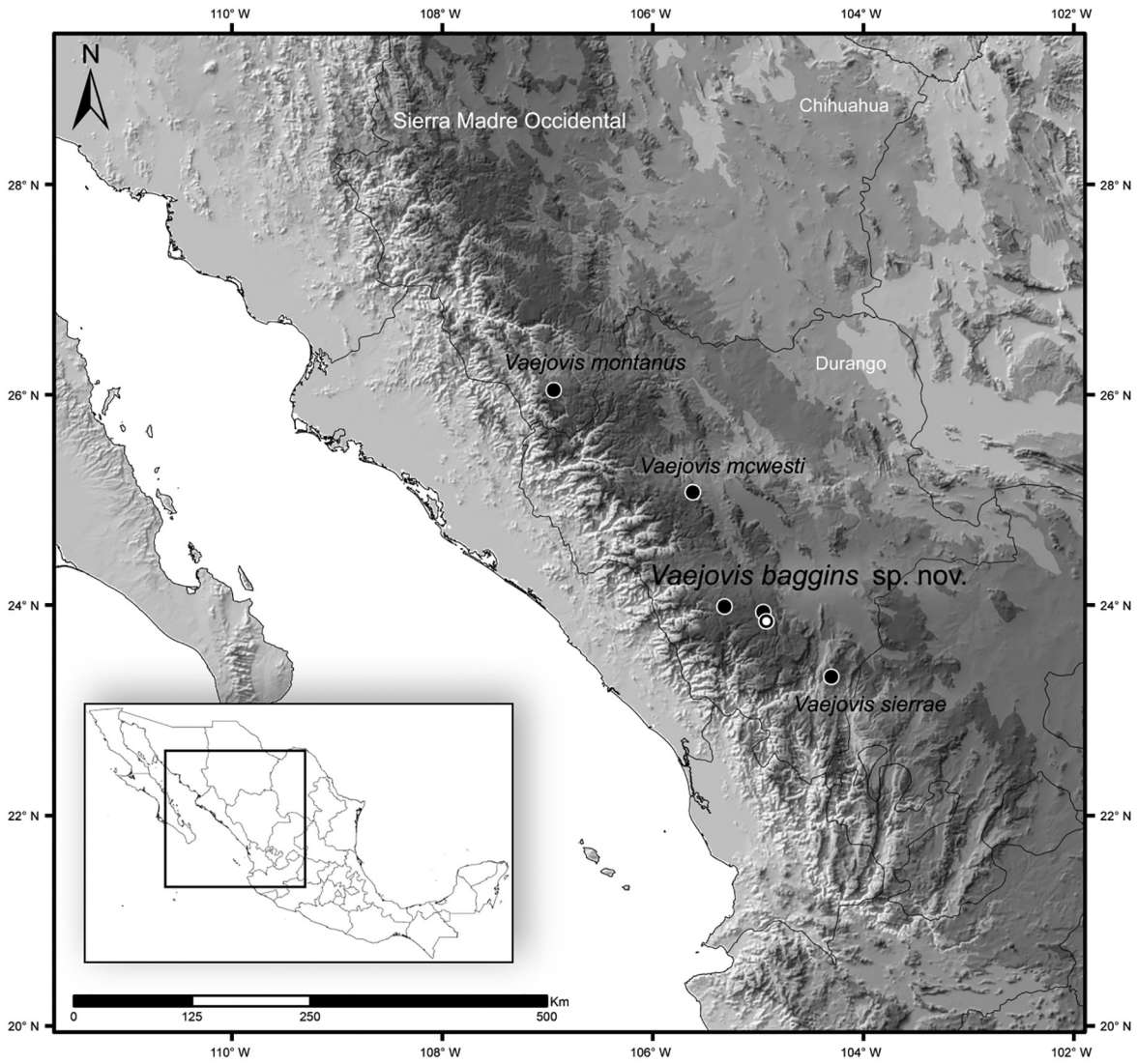

Figure 1. Type localities of species of the *mexicanus* group of *Vaejovis* C. L. Koch 1836 from the main massif of the Sierra Madre Occidental: *V. montanus* Graham and Bryson 2010, *V. sierrae* Sissom, Graham, Donaldson, and Bryson 2016, *V. mcwesti* Sissom, Graham, Donaldson, and Bryson 2016, and *V. baggins* **new species**. (white dot represents type locality; two black dots represent paratype localities).

These diagnostic characters include: (1) possession of six rows of denticles on the cutting margin of chela fixed finger; (2) basal position of trichobothria *ib – it* on the fixed finger; (3) possession of relatively robust pedipalps, particularly in the male; (4) a coloration pattern of fuscosity on a dark brown base color; (5) hemispermatophore with basally positioned capsular hooks; and (6) hemispermatophore with a median capsular lobe, but lacking a sclerotized mating plug [a more extensive diagnostic character list appears in Contreras-Félix and Francke (2019)]. A key that included the three species from the Sierra Madre Occidental provided in Sissom et al. (2016) is here updated to include the new species described in this paper.

Materials and Methods

Nomenclature follows Hjelle (1990); mensuration follows Sissom et al. (1990); trichobothrial designations follow Vachon (1974); pedipalp setation nomenclature follows Haradon (1984); metasomal setation nomenclature

follows Sissom et al. (2012); leg III setation nomenclature follows McWest (2009). Measurements were taken with an Olympus VM stereoscopic microscope calibrated with a micrometer at 2x. Hemispermatophores were dissected as described in Sissom et al. (1990) with the right hemispermatophore cleared in clove oil. Drawings were made utilizing photographs and observation of structures. Habitus photos were taken with a digital camera. Acronyms for museum depositories are as follows: AMNH, American Museum of Natural History, New York, New York, USA; CNAN, Colección Nacional de Áracnidos, Departamento de Zoología, Instituto de Biología, Universidad Nacional Autónoma de México, Mexico City, Mexico; UANL, Universidad Autónoma de Nuevo León, San Nicholas de los Garza, Nuevo León, Mexico.

Genetic data generated in a previous study (Bryson et al. 2013) were downloaded from the public repository GenBank (https://www.ncbi.nlm.nih.gov/genbank/), and augmented by new sequence data obtained for *V. mcwesti* from the type locality (accession numbers JX909597, JX909598, JX909601, JX909608, and JX909609). For these samples, a portion of the mitochondrial cytochrome c oxidase subunit I (COI) gene was amplified and sequenced using primers LE1r and COImodF and protocols outlined in Graham et al. (2019). Double-stranded DNA fragments were manually edited and aligned in GENEIOUS v7.1.9 (Biomatters Ltd, Auckland, New Zealand).

Sequence divergences among montane species of *Vaejovis* in the Sierra Madre Occidental were estimated using MEGA X v10.0.5 (Kumar et al. 2018). Phylogenetic relationships and divergence dates were simultaneously estimated using the criterion of Bayesian inference (BI) in BEAST v1.8.0 (Drummond et al. 2012). The best-fit substitution model was determined using MEGA X v10.0.5. An .xml file was generated in BEAUTi (BEAST package) using the best-fit substitution model (GTR+G), an uncorrelated lognormal clock model, and the Yule tree prior. Divergence times were estimated by calibrating the substitution rate for COI using upper and lower limits on the mean rate by uniform clock-rate priors of 0.00734 and 0.00393 substitutions/site/Myr, as estimated for vaejovids in Bryson et al. (2013). An initial run using an uncorrelated lognormal clock revealed a ucld.stdev value below 1.0 (mean = 0.324), which suggested clock-like sequence evolution. As such, a strict-clock model was implemented in final runs (as suggested in the BEAST manual). Two independent MCMC runs were conducted for 20 million generations and sampled every 20,000 generations. Markov chain stationarity and convergence, and appropriate effective sample sizes, were confirmed with TRACER v1.6 (Rambaut et al. 2014). The two runs were combined using TREEANNOTATOR (BEAST package) and visualized in FIGTREE v1.4.0 (http://tree.bio.ed.ac.uk/software/).

Vaejovis baggins Azzinnari, Bryson, Graham, Solís-Rojas, and Sissom

(Fig. 2–19, Table 1)

Type data. Holotype male (CNAN-T01428) from Rancho Santa Barbara, ca. 15 km S Hwy 40, Municipio Durango, Durango, Mexico (23°49.580′N, 104°54.896′W; 2245 m). 23 July 2013. R. W. Bryson Jr. and A. Huereca.

Paratypes. Same locality as holotype: 16 July 2010 (R. W. Bryson Jr., M. Torocco, and J. Jones), 10 adult females (CNAN-T01429); 23 July 2013 (R. W. Bryson Jr. and A. Huereca), five adult males, one subadult male (CNAN-T01430), two adult males, two adult females (UANL); Hwy 40 Durango–El Salto, km 91, Municipio Durango, Durango, Mexico (23°58.846′N, 105°19.155′W; 2446 m). 8 Aug 2005 (O.F. Francke, et al.), 1 adult male, 1 adult female (AMNH); Hwy 40 Durango–El Salto, km 45.5, Puente Mimbres, Municipio Durango, Durango, Mexico (23°55.605′N, 104°57.118′W; 2289 m), 8 Aug 2005 (O.F. Francke, et al.), 1 adult male (AMNH), 1 adult female (CNAN-T01431).

Etymology. This species epithet is a noun in apposition and based on the fictional character Bilbo Baggins in J.R.R. Tolkien's *The Hobbit* in reference to its small size.

Distribution. Known from three localities in the Sierra Madre Occidental southwest of Ciudad Durango in Durango, Mexico.

Diagnosis. *Vaejovis baggins* is most similar to *V. sierrae* and *V. mcwesti* from Durango and *V. montanus* from Chihuahua and Sonora. *Vaejovis baggins* differs from *V. sierrae* in the following ways: (1) *V. baggins* has a wider telson with the telson length to vesicle width ratio of males 2.37–2.68 and females 2.41–2.63, whereas *V. sierrae* has a ratio of 2.73 in the male holotype and a range of 2.71–2.83 in females; (2) *V. baggins* has a moderate basal tubercle

Figures 2–5. *Vaejovis baggins* **new species**, from Rancho Santa Barbara, Durango, Mexico. **2)** Ventral aspect, male holotype. **3)** Dorsal aspect, male holotype (CNAN-T01428). **4)** Ventral aspect, female paratype. **5)** Dorsal aspect, female paratype (CNAN-T01429). Scale line = 5 mm.

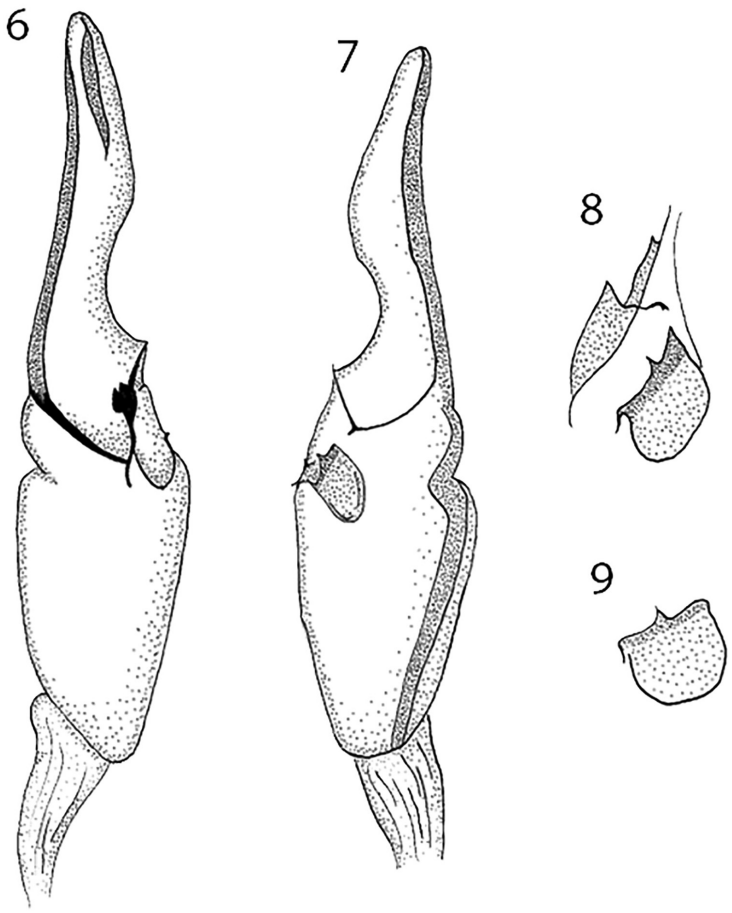

Figures 6–9. Right hemispermatophore of *Vaejovis baggins* **new species**. **6)** Dorsal surface of hemispermatophore. **7)** Ventral surface of hemispermatophore. **8)** Ectal view of midsection. **9)** Ectoventral aspect of capsular disk.

on the inner face of the pedipalp patella, whereas *V. sierrae* has a weak basal tubercle; (3) *V. baggins* has a moderate dorsointernal carina of the chela with several medium-sized granules and a few large granules, but it is weak with only a few granules in *V. sierrae*; (4) *V. baggins* has a weak dorsomarginal carina with more granules, whereas in *V. sierrae* it is weak and feebly granulose; (5) *V. baggins* most commonly has seven or more inner accessory denticles on the chela movable finger (43/44; 98%), whereas *V. sierrae* has six (9/14; 64%) or seven (5/14; 36%); (6) *V. baggins* most commonly has a setal count on the dorsolateral carinae of the metasoma of 0:0:1:1 (39/44; 89%), whereas *V. sierrae* most commonly has a setal count of 0:0:0:1 (12/14; 86%); and (7) *V. baggins* has 1–6 setae on each side when totaling all of the setae on the lateral inframedian carinae of metasoma I–IV, whereas *V. sierrae* is limited to one or two in total. The localities of *V. baggins* along Hwy 40 southwest of Ciudad Durango are also separated from the mountain range with *V. sierrae* by the Rio Mezquital drainage (Fig. 1). This river drainage is a formidable barrier to many codistributed montane taxa (Bryson et al. 2012).

Vaejovis baggins differs from *V. mcwesti* in the following ways: (1) *V. baggins* has more slender pedipalp chela with a length to width ratio of 3.26–3.79 in males and 3.52–3.86 in females, whereas *V. mcwesti* has a ratio of 3.16 in the holotype male and a range of 3.25–3.42 in females; (2) *V. baggins* females have a wider telson with the telson length to vesicle width ratio 2.41–2.63, whereas *V. mcwesti* has a ratio of 2.64–2.77; (3) *V. baggins* has approximately 20 granules on the internal face of the pedipalp femur, whereas *V. mcwesti* has approximately eight; (4) *V. baggins* has a granular dorsolateral carinae on metasoma V, whereas *V. mcwesti* is serrate anteriorly; (5) *V. baggins* most commonly has three setae on the ventral submedian carinae of metasoma IV (40/44; 91%), whereas *V. mcwesti* has four or more (11/12; 92%); (6) *V. baggins* has a 1+2 (29/44; 66%) or 2+2 (15/44; 34%)

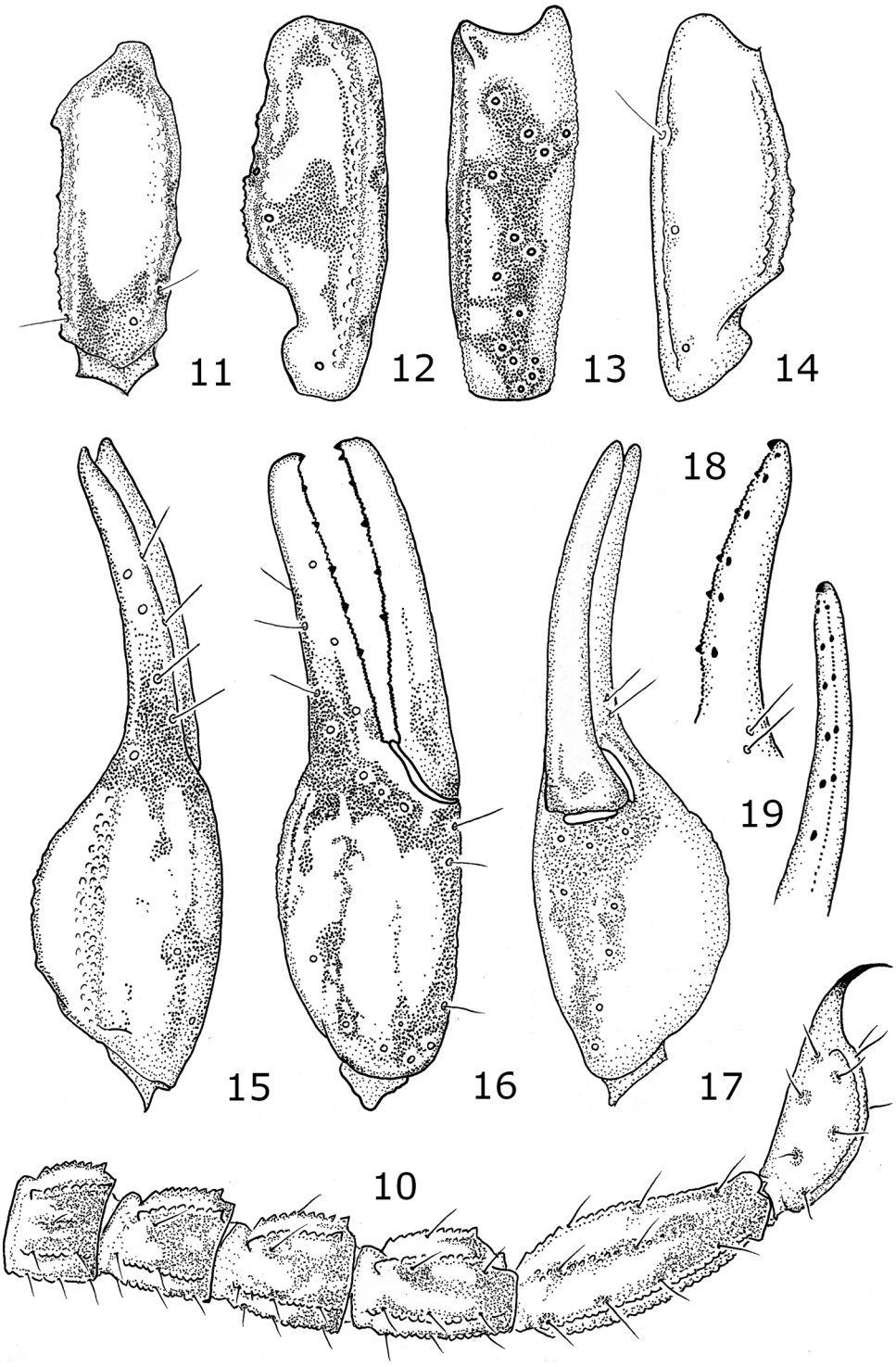

Figures 10–19. Morphology of *Vaejovis baggins* **new species**, based on male holotype. **10)** Lateral view of metasoma and telson. **11)** Right pedipalp femur, dorsal. **12)** Right pedipalp patella, dorsal. **13)** Right pedipalp patella, external. **14)** Right pedipalp patella, ventral. **15)** Right pedipalp chela, dorsal. **16)** Right pedipalp chela, external. **17)** Right pedipalp chela, ventral. **18)** Apposable dentate margin of chela fixed finger. **19)** Apposable dentate margin of chela movable finger.

Table 1. Ranges, means, and standard deviations for selected measurements of male (n = 9) and female (n = 13) *Vaejovis baggins* **new species**. Abbreviations: L = length, W = width, D = depth, FF = pedipalp chela fixed finger, MF = pedipalp chela movable finger, Ped = pedipalp, Fem = femur, Met = metasomal segment, Ca = carapace, S.D. = standard deviation. Note: The aculeus was broken on two females and one male, and telson measurements were not taken on them.

Structure	Sex	Range	Mean ± S.D.
Ca L	♂	2.33–2.83	2.62 ± 0.14
	♀	2.86–3.29	3.03 ± 0.12
Met III L	♂	1.06–1.42	1.30 ± 0.10
	♀	1.34–1.50	1.42 ± 0.06
Met III W	♂	1.21–1.47	1.37 ± 0.08
	♀	1.44–1.67	1.55 ± 0.07
Met V L	♂	2.28–3.03	2.72 ± 0.21
	♀	2.80–3.19	2.99 ± 0.12
Met V W	♂	1.14–1.34	1.28 ± 0.06
	♀	1.35–1.57	1.48 ± 0.06
Ped Fem L	♂	1.67–2.22	2.01 ± 0.16
	♀	2.17–2.38	2.28 ± 0.08
Ped Fem W	♂	0.61–0.76	0.70 ± 0.04
	♀	0.76–0.91	0.83 ± 0.05
Ped Chela L	♂	2.93–3.94	3.59 ± 0.29
	♀	3.89–4.35	4.11 ± 0.13
Ped Chela W	♂	0.81–1.15	1.02 ± 0.09
	♀	1.06–1.21	1.12 ± 0.05
FF L	♂	1.42–1.85	1.72 ± 0.14
	♀	1.85–2.10	1.98 ± 0.07
MF L	♂	1.77–2.38	2.15 ± 0.18
	♀	2.33–2.60	2.47 ± 0.08
Telson L	♂	2.28–2.98	2.76 ± 0.23
	♀	2.81–3.26	3.11 ± 0.13
Telson W	♂	1.14–1.34	1.28 ± 0.06
	♀	1.16–1.29	1.23 ± 0.04

setal arrangement flanking the ventromedian carinae of metasoma V, whereas *V. mcwesti* most commonly has a 2+2 (4/12; 33%), 3+2 (3/12; 25%), or 4+2 (3/12; 25%) arrangement; and (7) *V. baggins* has a few granules on the ventrointernal carina on the chela, whereas it remains a smooth ridge in *V. mcwesti*.

Vaejovis baggins differs from *V. montanus* in the following ways: (1) *V. baggins* is a smaller species with males ranging 18.56–22.03 mm (n = 8) and females ranging 21.97–26.25 mm (n = 12) in length where *V. montanus* males are larger than 26.00 mm and some females (n = 4) exceed 28.00 mm in length; (2) *V. baggins* has pedipalp carinae that is weaker and less granulose than *V. montanus*; (3) the lateral and ventral intercarinal surfaces of metasoma IV and V, as well as the underside of the telson, have only a few granules in *V. baggins* but are moderately to densely granular in *V. montanus*; (4) *V. baggins* has weaker metasomal carinae; and (5) *V. baggins* has a 1 + 2 (29/44; 66%) or 2 + 2 (15/44; 34%) setal arrangement on the ventromedian carinae of metasoma V, whereas *V. montanus* most commonly has two to four anterior setae.

Description. The following description is based on the holotype male.

Coloration. Carapace and tergites dark brown, with distinct pattern of dusky markings (Fig. 2–3). Metasomal segments dark brown; dorsal markings limited to posterior ends of carinae and small dark spots in dorsal intercarinal spaces; lateral fuscosity more extensive, associated with the carinae, setal pits, and intercarinal spaces; ventral fuscosity limited to carinae and setal pits; metasoma V with heavier fuscosity in posterior half. Telson orange brown with a few small dorsal and lateral dusky spots; aculeus dark reddish brown. Cheliceral manus light orange brown, dorsally with distal edge and movable finger bearing dusky markings; cheliceral teeth dark brown. Pedipalp femur and patella orange brown with small amounts of fuscosity located at or near trichobothrial setal pits. Pedipalp chela orange brown with fuscous spots surrounding trichobothria and setal pits and a band of fuscosity at distal end of manus which extends well onto fixed finger. Carinae of pedipalps and metasoma dark brown to reddish brown. Coxosternal region and sternites III–VI yellow brown, unmarked; sternite VII yellow brown with light fuscosity on posterior edge. Legs lighter yellow brown with strong fuscosity.

Prosoma. Carapace length slightly greater than posterior width; ratio of carapace L/metasomal segment V length 0.96. Median ocular prominence slightly raised above carapacial surface. Two macrosetae anterior to eyes on ocular prominence. Anterior margin obtusely emarginate; median notch rounded. Carapace densely finely

granular, with scattered coarse granulation associated with fuscous areas. Posterior margin strongly fuscous. Three pairs of evenly spaced macrosetae on posterior margin.

Mesosoma. Longitudinal median carina absent on tergites I–II; on III–VI represented by faint granular ridges. Tergite VII with median carina present, weak on anterior half, granular; both pairs of lateral carinae strong, serratocrenulate. Pre-tergites densely finely granular; post-tergites densely, finely granular with scattered coarse granulation in fuscous areas. Pectinal teeth numbering 14/14. Sternite III with two anterior medial macrosetae and a transverse, row of four macrosetae near midsegment; sternites IV–VI with two macrosetae anterior to each book lung spiracle (lateral macroseta missing on left side of sternite VI) and a transverse, recurved row of four macrosetae near mid-segment; sternite VII with three pairs of lateral setae (two of these on lateral carina) and one pair of medial setae; all five sternites with regularly spaced lateral and posterior marginal macrosetae. Sternite V with an inconspicuous medial pale patch along posterior margin; anterior edge of patch evenly convex. Sternites III–VII shagreened medially, with granulation laterally (stronger and denser on posterior sternites). Sternite VII with one pair of weak, granular lateral carinae that weakens anteriorly.

Hemispermatophore (Fig. 6–9). Lamelliform with strong dorsal crest on distal lamina extending approximately one-third the length of the blade; distal lamina with basal constriction, widening at middle, and distinctly tapering distally. Two dorsal "hooks" positioned just above the dorsal trough, with ectal hook distinctly larger. Ventral capsular area with a flat, rounded plate bearing a sharp prong which projects ectally.

Metasoma (Fig. 10). Segment I length/width ratio 0.71, III length/width ratio 0.93, V length/width ratio 2.11. Segments I–IV: Dorsolateral carinae strong, irregularly serratocrenulate on I, crenulate on II–IV; terminal denticles distinctly enlarged, spinoid. Lateral supramedian carina on I strong, serratocrenulate, on II–IV strong, crenulate; terminal denticles enlarged, spinoid on I–III, flared on IV. Lateral inframedian carinae on I strong, complete, granulose on left, crenulate on right; on II present on posterior one-half, stronger posteriorly, crenulate; on III present on posterior one-quarter, stronger posterior, crenulate; on IV absent. Ventrolateral carinae on I moderate, serratocrenulate; on II–IV strong, serratocrenulate. Ventral submedian carinae on I weak, granular; on II moderate, crenulate; on III–IV strong, crenulate. Intercarinal spaces densely, finely granular with a few scattered coarse granules in fuscous areas. Segment V: Dorsolateral carinae stronger anteriorly, granulose. Lateromedian carinae moderate basally, weak distally; present on anterior three-fourths, granulose. Ventrolateral and ventromedian carinae strong, serrate. Intercarinal surfaces densely finely granular, with a few coarse granules ventrally in fuscous areas. Metasomal I–IV carinal setation (Fig. 10): dorsolaterals, 0/0:0/0:1/1:1/1; lateral supramedians, 0/0:1/1:1/1:2/2; lateral inframedians, 1/1:0/0:0/0:0/0; ventrolaterals, 2/2:2/2:3/3:3/3; ventral submedians, 3/3:3/3:3/3:3/4; ventromedian intercarinal spaces lacking accessory setae. Setation of metasomal segment V: dorsolaterals, 3/3; lateromedians, 2/2; ventrolaterals, 4/4; ventromedians, 1/1 + 2/2.

Telson (Fig. 10). Moderately slender, distinctly narrower than metasoma V and with length/depth ratio 3.11. Dorsal surface of vesicle slightly bulged. Underside of vesicle with eight pairs of macrosetae and several smaller paired setae. Ventral aspect of telson with sparse, scattered granulation.

Chelicera. Movable finger dorsally with one large distal tine, two smaller subdistal tines, one large medial tine, and one small basal tine. Ventral margin of cheliceral movable finger with well-developed serrula.

Pedipalp. Trichobothrial pattern, Type C, orthobothriotaxic (Fig. 11–19). Femur (Fig. 11): length/width ratio 2.99. Tetracarinate: dorsointernal carina moderate, irregularly crenulate; dorsoexternal carinae moderate, granulose; ventrointernal carina moderate, crenulate; ventroexternal carina weak, granular. All faces densely, finely granular; internal face additionally with about 20 larger, irregularly spaced, rounded granules. Internal face with one supramedial macroseta and three inframedial macrosetae; external face with two medial macrosetae. Patella (Fig. 12–14): length/width ratio 2.73. Pentacarinate. Dorsointernal carina moderate, irregularly crenulate; internomedian carina oblique, moderate, irregular with several large granules and a few small granules, with pronounced basal tubercle**;** ventrointernal carina moderate, serrate; dorsoexternal and ventroexternal carinae moderate, granular. All faces densely, finely granular. Internal face with 2 supramedial and 2 inframedial macrosetae. Proximal slope to the basal tubercle relatively steep. Chela (Fig. 15–19): dorsal marginal carina weak and granulose; dorsal secondary, digital, and external secondary carinae represented by faint, smooth, rounded ridges; dorsointernal carina moderate, with several medium-sized granules and some large granules; ventrointernal carina weak, with a few small granules; ventroexternal carinae weak, granular; ventromedian absent. Intercarinal surfaces densely, finely granular. Dentate margin of fixed finger (Fig. 18) with primary denticle row

divided into six subrows by five enlarged denticles; seven inner accessory denticles. Dentate margin of movable finger (Fig. 19) with primary row divided into six subrows by five enlarged denticles; apical subrow consisting of a single small denticle; seven inner accessory denticles. Dentate margins of chela fingers straight in lateral profile. Chela length/width ratio 3.56; fixed finger length/carapace length ratio 0.67.

Leg. Right telotarsus III with ventromedian spinule row terminating between a single pair of slightly offset spinules; left telotarsus III terminating between a pair of enlarged spinules; fourteen macrosetae on left and fifteen macrosetae on right (excluding superoterminal landmark macroseta) as follows (L/R): *ri* 1/1, *rid* 1/1, *rit* 1/1, *rm* 1/2, *rmt* 1/1, *rs* 1/1, *rst* 1/1, *pi* 1/1, *pid* 1/1, *pit* 1/1, *pm* 1/2, *pmt* 1/1, *ps* 1/1, *pst* 1/1 (after McWest 2009).

Measurements of male holotype (mm). Total L (additive), 20.35; carapace L, 2.73; mesosoma L, 6.17; metasoma L (additive), 8.47; telson L, 2.98. Metasomal segments: I L/W, 1.16/1.64; II L/W, 1.29/1.52; III L/W, 1.37/1.47; IV L/W, 1.82/1.42; V L/W, 2.83/1.34. Telson: vesicle L/W/D, 1.87/1.16/0.96; aculeus L, 1.11. Pedipalps: femur L/W, 2.12/0.71; patella L/W, 2.35/0.86; chela L/W/D, 3.77/1.06/1.16; fixed finger L, 1.82; movable finger L, 2.28; palm (underhand) L, 1.67.

Measurements of female paratype (mm). Total L (additive), 22.78; carapace L, 3.13; mesosoma L, 7.38; metasoma L (additive), 9.10; telson L, 3.16. Metasomal segments: I L/W, 1.21/1.79; II L/W, 1.39/1.69; III L/W, 1.47/1.62; IV L/W, 1.92/1.57; V L/W, 3.13/1.52. Telson: vesicle L/W/D, 1.92/1.26/0.94; aculeus L, 1.24. Pedipalps: femur L/W, 2.38/0.88; patella L/W, 2.65/1.01; chela L/W/D, 4.30/1.14/1.26; fixed finger L, 2.10; movable finger L, 2.58; palm (underhand) L, 1.87.

Variation. Variation in morphometric characters for both males and females is summarized in Tables 1 and 2. The 13 female specimens exhibited pectinal tooth counts as follows: there was one comb with 10 teeth, 16

Table 2. Ranges, means, and standard deviations for selected morphometric ratios of male (n = 9) and female (n = 13) *Vaejovis baggins* new species. Abbreviations: L = length, W = width, D = depth, FF = pedipalp chela fixed finger, MF = pedipalp chela movable finger, Ped = pedipalp, Fem = femur, Met = metasomal segment, Ca = carapace, S.D. = standard deviation. Note: The aculeus was broken on two females and one male, and the telson length/width ratio was not calculated for them.

Ratio	Sex	Range	Mean ± S.D.
Ped Chela L/W	♂	3.26–3.79	3.52 ± 0.18
	♀	3.52–3.86	3.69 ± 0.13
Ped Femur L/W	♂	2.75–3.00	2.89 ± 0.09
	♀	2.61–2 .87	2.72 ± 0.08
MF L/Ped Chela	♂	1.95–2.32	2.11 ± 0.13
	♀	2.08–2.33	2.21 ± 0.08
FF L/Ca L	♂	0.61–0.70	0.66 ± 0.02
	♀	0.62–0.68	0.65 ± 0.02
Met III L/W	♂	0.88–1.04	0.95 ± 0.04
	♀	0.88–1.03	0.92 ± 0.05
Met V L/W	♂	2.00–2.26	2.12 ± 0.09
	♀	1.90–2.07	2.02 ± 0.05
FF L/Ped Chela L	♂	0.47–0.49	0.48 ± 0.01
	♀	0.46–0.50	0.48 ± 0.01
Ca L/Met V L	♂	0.91–1.02	0.96 ± 0.04
	♀	0.98–1.05	1.02 ± 0.02
Telson L/W	♂	2.37–2.68	2.56 ± 0.10
	♀	2.41–2.63	2.53 ± 0.07

combs with 12 teeth, eight combs with 13 teeth, and one comb with 14 teeth. The nine male specimens exhibited pectinal tooth counts as follows: there were 13 combs with 14 teeth, and five combs with 15 teeth.

All the specimens had six denticle subrows and inner accessory denticles on the chela fixed finger (n = 43 fingers) except for one that could not be counted. All specimens had six denticle subrows on the chela movable finger (n = 44 fingers). Nineteen of the 21 specimens had seven inner accessory denticles, one had eight with the 6th denticle doubled, and one had five.

There was no observed variation in the numbers of macrosetae on the pedipalp femur (internal supramedials and inframedials; external medians) and patella (internal supramedians and inframedians). There was some variation in metasomal segments I–IV setal counts (n = 44 carinae), as follows: dorsolaterals, 0:0:0:1 (n = 3; 6.82%), 0:0:1:1 (n = 39; 88.64%), 0:1:1:1 (n = 2; 4.55%); lateral supramedians, 0:1:1:1 (n = 1; 2.27%), 0:1:1:2 (n = 43; 98.73%); lateral inframedians, 1:0:0:0 (n = 17; 38.64%), 1:0:0:1 (n = 4; 9.09%), 1:0:1:0 (n = 1; 2.27%), 1:1:0:0 (n = 3; 6.82%), 2:0:0:0 (n = 2; 4.55%), 2:0:0:1 (n = 1; 2.27%), 2:0:1:0 (n = 2; 4.55%), 2:1:0:1 (n = 1; 2.27%), 2:1:1:0 (n = 1; 2.27%), 2:1:1:1 (n = 7; 15.91%), 3:1:1:1 (n = 6; 6.82%); ventrolaterals, 2:2:2:3 (n = 1; 2.27%), 2:2:3:3 (n = 6; 13.64%), 2:3:2:3 (n = 2; 4.55%), 2:3:3:3 (n = 35; 79.55%); and ventral submedians I–IV, 3:2:3:3 (n = 2; 4.55%), 3:3:3:3 (n = 38; 86.36%), 3:3:3:4 (n = 4; 9.09%). All specimens had no accessory setae except for one on metasoma IV. For segment V: dorsolaterals, 3 (n = 41; 93.18%), 4 (n = 3; 6.82%); lateromedians, 2 (n = 24; 54.55%), 3 (n = 20; 45.45%); ventrolaterals, 3 (n = 1; 2.27%), 4 (n = 38; 86.36%), 5 (n = 4' 9.09%), 6 (n = 1; 2.27%); the ventromedian carinae bore 2+2 (n = 15; 34.09%) or 1+2 macrosetae (n = 29; 65.91%).

Two more hemispermatophores were dissected, and one lacked the dorsal crest on the blade whereas the other matched the morphology of the first.

Genetic comparisons. The uncorrected pairwise sequence divergence between *V. baggins* and other *Vaejovis* in the Sierra Madre Occidental ranged from 8.10% (*V. baggins* vs *V. sierrae*) to 6.73% (*V. baggins* vs *V. mcwesti*). Phylogenetic analyses of mitochondrial DNA (Fig. 20) placed *V. baggins* and *V. mcwesti* together in a clade that was divergent from the southern species *V. sierrae*, consistent with the expectation that the low-elevation Mezquital

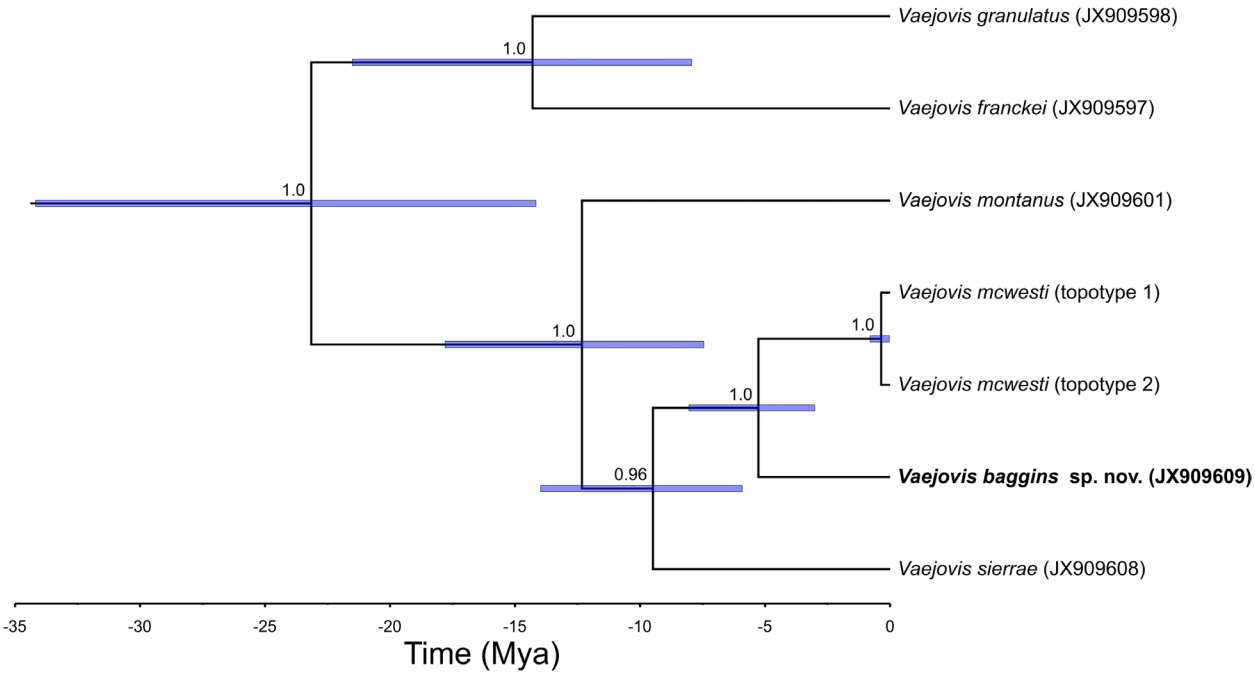

Figure 20. Time-calibrated mitochondrial phylogeny showing the relationship of *Vaejovis baggins* **new species** to other species of montane *Vaejovis* from the Sierra Madre Occidental. Posterior probabilities indicated at nodes. Bars represent highest posterior densities (95%) around mean date estimates. GenBank accession numbers are provided in parentheses.

River drainage may be acting as a filter barrier to highland taxa (Bryson et al. 2011, 2012). *Vaejovis baggins* and *V. mcwesti* were estimated to have shared a common ancestor during the late Miocene or Pliocene (3–8 Mya; Fig. 20). Based on mean estimated divergence dates, the montane species of *Vaejovis* in the Sierra Madre Occidental likely diverged around 5–13 Mya (Fig. 20).

Key to the Species of the *Vaejovis mexicanus* group from the Sierra Madre Occidental

1. Dorsal marginal, digital, dorsal secondary, ventroexternal, and dorsointernal carinae of pedipalp chelae well developed, granular to granulose . . . . . ***V. montanus* Graham and Bryson, 2010**

— Pedipalp chela with carinae poorly developed with weaker granulation **2**

2(1). Weak basal tubercle on pedipalp patella; dorsolateral carinae of metasomal segments I–IV 0:0:0:1 . . . . . ***V. sierrae* Sissom, Graham, Donaldson, and Bryson, 2016**

— Strong basal tubercle on pedipalp patella; dorsolateral carinae of metasoma segments I–IV 0:0:1:1 . . . **3**

3(2). Pedipalp more robust, with chela length/width ratio 3.16 in known male, 3.25–3.42 in known females; granules of internal face of pedipalp femur numbering around 8; dorsolateral carinae on metasoma V serrate anteriorly; four or more setae on the ventral submedian carinae of metasoma IV . . . . . ***V. mcwesti* Sissom, Graham, Donaldson, and Bryson, 2016**

— Pedipalp more slender, chela length/width ratio 3.26–3.79 in males and 3.52–3.86 in females; granules of internal face of pedipalp femur numbering around 20; dorsolateral carinae on metasoma V granular throughout; three, rarely four, setae on the ventral submedian carinae of metsoma IV . . . . . ***V. baggins* Azzinnari, Bryson, Graham, Solís-Rojas, and Sissom, new species.**

Acknowledgments

We thank L. Prendini (AMNH) and O. F. Francke (CNAN) for the loan of material supporting this research; J. Ballesteros, C. Duran-Barron, O. F. Francke, A. Huereca, L. Jarvis, J. Jones, C. M. Lee, K. J. McWest, H. Montaño, and M. Torocco for their collaboration and assistance in the field; O. F. Francke for assistance in securing collecting permits; and O. F. Francke and B. E. Hendrixson for reviewing the manuscript. This research was supported in part by NSF BIO-DEB 0413453 grant to L. Prendini of the American Museum of Natural History.

Literature Cited

Bryson RW Jr., García-Vázquez UO, Riddle BR. 2012. Diversification in the Mexican horned lizard *Phrynosoma orbiculare* across a dynamic landscape. Molecular Phylogenetics and Evolution 62: 87–96.

Bryson RW Jr., Murphy RW, Lathrop A, Lazcano-Villareal D. 2011. Evolutionary drivers of phylogeographical diversity in the highlands of Mexico: a case study of the *Crotalus triseriatus* species group of montane rattlesnakes. Journal of Biogeography 38: 697–710.

Bryson RW Jr., Riddle BR, Graham MR, Smith BT, Prendini L. 2013. As old as the hills: Montane scorpions in southwestern North America reveal ancient associations between biotic diversification and landscape history. PLoS ONE 8: e52822.

Contreras-Félix GA, Francke OF. 2019. Taxonomic revision of the "*mexicanus*" group of the genus *Vaejovis* C. L. Koch, 1836 (Scorpiones: Vaejovidae). Zootaxa 4596: 1–100.

Drummond AJ, Suchard MA, Xie D, Rambaut A. 2012. Bayesian phylogenetics with BEAUti and the BEAST 1.7. Molecular Biology and Evolution 29: 1969–1973.

Ferrusquía-Villafranca I, González-Guzmán LI, Cartron J-LE. 2005. Northern Mexico's landscape, part I: the physical setting and constraints on modeling biotic evolution. p. 39–41. In: Cartron JLE, Ceballos G, Felger RS (eds.). Biodiversity, ecosystems, and conservation in northern Mexico. Oxford University Press; NY. 514 p.

Graham MR, Bryson RW Jr. 2010. *Vaejovis montanus* (Scorpiones: Vaejovidae), a new species from the Sierra Madre Occidental of Mexico. The Journal of Arachnology 38: 285–293.

Graham MR, Myers EA, Kaiser RC, Fet V. 2019. Cryptic species and co-diversification in sand scorpions from the Karakum and Kyzylkum deserts of Central Asia. Zoologica Scripta 48: 801–812.

Haradon RM. 1984. New and redefined species belonging to the *Paruroctonus borregoensis* group (Scorpiones, Vaejovidae). Journal of Arachnology 12: 317–339.

Hjelle JT. 1990. Chapter 2: Anatomy and morphology. p. 9–63. In: Polis GA (ed.). The biology of scorpions. Stanford University Press; Stanford, CA. 587 p.

Hoffmann CC. 1931. Los scorpiones de México. Primera Parte. Anales del Instituto de Biología de la Universidad Nacional Autónoma de México 2: 291–408.

Kumar S, Stecher G, Li M, Knyaz C, Tamura K. 2018. MEGA X: molecular evolutionary genetics analysis across computing platforms. Molecular Biology and Evolution 35: 1547–1549.

McWest KJ. 2009. Tarsal spinules and setae of vaejovid scorpions (Scorpiones: Vaejovidae). Zootaxa 2001: 1–126.

Rambaut A, Suchard MA, Xie D, Drummond AJ. 2014. Tracer v1.6. Available at http://beast.bio.ed.ac.uk/Tracer (Last accessed March 15, 2020.)

Sissom WD. 2000. Family Vaejovidae. p. 503–553. In: Fet V, Sissom WD, Lowe G, Braunwalder ME (eds.). Catalog of the scorpions of the world (1758–1998). New York Entomological Society; NY. 690 p.

Sissom WD, Graham MR, Donaldson TG, Bryson RW Jr. 2016. Two new *Vaejovis* CL Koch 1836 from highlands of the Sierra Madre Occidental, Durango, Mexico (Scorpiones, Vaejovidae). Insecta Mundi 0477: 1–14.

Sissom WD, Hughes GB, Bryson RW Jr., Prendini L. 2012. The *vorhiesi* group of *Vaejovis* C.L. Koch, 1836 (Scorpiones: Vaejovidae) in Arizona, with description of a new species from the Haulapai Mountains. American Museum Novitates 3472: 1–19.

Sissom WD, Polis GA, Watt DD. 1990. Chapter 11: Field and laboratory methods, p. 445–461. In: Polis GA (ed.). The biology of scorpions. Stanford University Press; Stanford, CA. 588 p.

Vachon M. 1974. Étude des caractères utilisés pour classer les familles et les genres de Scorpions (Arachnides). 1. La trichobothriotaxie en Arachnologie, Sigles trichobothriaux et types de trichobothriotaxie chez les Scorpions. Bulletin du Muséum National d'Histoire Naturelle, Paris, (3), 140 (Zool. 104), mai-juin 1973: 857–958.

Received November 5, 2020; accepted January 11, 2021.
Review editor Lawrence Hribar.